Photocatalytic generation of H_2 gas from neat ethanol over Pt/TiO_2 nanotube catalysts

C.-H. Lin[1]*, C.-H. Lee[2], J.-H. Chao[3], C.-Y. Kuo[1], Y.-C. Cheng[1], W.-N. Huang[1], H.-W. Chang[2], Y.-M. Huang[1], and M.-K. Shih[1]

[1]*Department of Chemistry, National Changhua University of Education, Changhua 500, Taiwan*
[2]*Department of Engineering and System Science, National Tsing Hua University, Hsinchu 300, Taiwan*
[3]*Nuclear Science and Technology Development Center, National Tsing Hua University, Hsinchu 300, Taiwan*

Received 27 February 2004; accepted 22 July 2004

TiO_2 nanotubes promoted with Pt metal were prepared and tested to be the photocatalytic dehydrogenation catalyst in neat ethanol for producing H_2 gas ($C_2H_5OH \rightarrow C_3CHO + H_2$). It was found that the ability to produce H_2, the liquid phase product distribution and the catalyst stability of these promoted nano catalysts all depended on the Pt loading and catalyst preparation procedure. These Pt/TiO_2 catalysts with TiO_2 nanotubes washed with diluted H_2SO_4 solution produced 1, 2-diethoxy ethane (acetal) as the major liquid phase product, while over those washed with diluted HCl solution or H_2O, acetaldehyde was the major liquid phase product.

KEY WORDS: dehydrogenation, ethanol, hydrogen, photocatalytic, TiO_2 nanotube.

1. Introduction

Recently, there has been a huge interest in the development of the nanotechnology and its applications in heterogeneous catalysis [1,2]. Although from the early stage of the development of heterogeneous catalysis, many heterogeneous catalytic processes utilize particles in nanometer-size range as catalysts, in which small metal particles supported on a porous support were used to catalyze various reactions such as hydrogenation (Ni), catalytic reforming (Pt), epoxidation (Ag), and selective oxidation (Ag). At the time (to just a few years ago), high dispersion instead of nanometer-size was used to describe the state of the metal particles. Nonetheless, the robust research progress made by the nanotechnology is extremely beneficial for both understanding and improving the catalyst performance at the molecular scale. At the same time, it also provides us with great opportunities for discovering new catalysts. For example, Au has traditionally been regarded as an inert metal, on which the adsorption of the reactive molecules such as H_2 and O_2 can hardly occur and the catalytic hydrogenation and oxidation reactions are unable to proceed. Interestingly, nanometer-size Au particles dispersed on an anatase TiO_2 displayed exceptional activity toward CO oxidation even at ambient temperature [3] and at very low pressure (6.7×10^{-5} Pa) [4]. In addition, there was a recent report that Pt nanowire (2.5 nm in diameter and 50–300 nm in length) prepared by photoreduction of H_2PtCl_6 supported on FSM-16 showed a much higher catalytic activity than Pt particles (2.5 nm in diameter) supported on the same FSM-16 prepared by H_2 reduction at 673 K in water-gas shift reaction. This Pt nanowire also exhibited unique properties in CO chemisorption and magnetism due to its morphology in the mesoporous channel of FSM-16 [5].

Recently, our laboratory was able to prepare grams-quantity of highly pure TiO_2 nanotubes per synthesis run with a simple chemical processing method utilizing TiO_2 powder in a hot concentrated NaOH solution [6]. SEM reveals that these TiO_2 nanotubes have an outer diameter distribution between 10 and 100 nm and an average tube length of > 10 μm. Low temperature adsorption of N_2 indicates that these nanotubes have an inner free diameter of 30–40 nm, a BET surface area of 250–300 m^2/g and a total pore volume of 0.88 mL/g. Furthermore, XRD data suggest that these TiO_2 nanotubes may consist of small anatase phase grains. It is quite exciting that this material has a high surface area and a large one-dimensional mesopore/macropore. These properties make them a suitable candidate to be utilized as a catalyst or catalyst support for the liquid phase reactions.

In order to develop a green production technology for generating H_2 gas, photodehydrogenation of neat ethanol at ambient temperature and pressure (equation (1)) over Pt/TiO_2 catalyst seems to be an ideal system [7–18]. Such catalyst system harvests UV-ray in the solar energy and transforms it into chemical energy at ambient temperature and pressure. Furthermore, it utilizes a non-toxic and renewable raw material such as ethanol, and produces H_2 fuel and acetaldehyde as the reaction products. Hydrogen gas produces generous amount of energy and non-polluting H_2O after

* To whom correspondence should be addressed.
E-mail: chlin@cc.ncue.edu.tw

1011-372X/04/1000–0061/0 © 2004 Plenum Publishing Corporation

combustion, and eliminates the production of green house gas, CO_2. Acetaldehyde is a useful intermediate for manufacturing numerous chemical products. From the point of view of practicing the green chemistry, the reaction is truly 100% atom economy.

$$C_2H_5OH \rightarrow CH_3CHO + H_2 \quad (1)$$

In this paper, we have explored the possibility to develop a photocatalyst based on our newly synthesized TiO_2 nanomaterial. Our preliminary data show that these Pt-promoted TiO_2 nanotubes were indeed able to produce H_2 gas, but both Pt loading and the catalyst preparation procedure have a significant effect on the activity, product distribution and life of such photocatalyst.

2. Experimental

1.0 g of anatase TiO_2 powder (Aldrich) was mixed with 300 mL of 10 M NaOH solution in a perfluoroalkoxy container and stirred for 7 days at 383 K. The resulting paste was filtered, washed with deionized water, neutralized with 0.1 M HCl or 0.05 M H_2SO_4 solution. These washed samples were filtered and dried at 383 K for 24 h, and sieved with 40 mesh screen to obtain TiO_2 nanotube samples. To induce the acidity in these TiO_2 nanotubes, the samples washed with 0.05 M H_2SO_4 was calcined at 573 K in air for 3 h at a heating rate of 1 K/min. To prepare Pt/TiO_2 nanotube catalyst, TiO_2 nanotube sample was placed in 500 mL 1:1 volume ratio of aqueous methanol containing calculated amount of H_2PtCl_6. Such suspension solution was purged with argon gas for 30 min and irradiated with 365 nm UV-ray (UVP) for 24 h (photodeposition method). After irradiation, the suspension solution was filtered to obtain a sample with dark-gray color. This dark-gray sample was washed several times with deionized water until no Cl^- was detected with 0.1 M $AgNO_3$ solution and dried at 383 K to obtain Pt/TiO_2 nanotube catalyst.

SEM images of the nanotubes were obtained with a Hitachi S-2460N scanning electron microscope. The Pt and Na^+ content in TiO_2 nanotubes were estimated by the ICP-AES on the digested samples. BET surface areas were obtained with an ASAP 2010 surface area and porosimetry analyzer. UV-visible absorption spectra of Pt/TiO_2 catalysts were obtained for the dry pressed disk samples using UV-visible spectrometer (HP-8453) between 200 and 900 nm. TPD/NH_3 experiments were performed with on a Autochem 2910 automated catalyst characterization system (Micromeritics) interfaced with qudrapole mass spectrometer (Proleb, Thermo Onix). XRD spetra were obtained with Shimadzu Lab-X XRD-6000 using Fe Kα as the X-ray source (λ = 1.93604A).

Temperature programmed desorption (TPD) experiments using ammonia as adsorbate and a qudrapole mass spectrometer as the detector were performed on the catalysts to compare their acidity. Before introducing NH_3, 50 mg of catalyst was dried at 573 K for 3 h in air flowing at a rate of 30 mL min^{-1}. The adsorption step was conducted at 100 °C using a flowing NH_3 of 30 mL min^{-1} for 30 min. After adsorption, the gas flow was switched to 30 mL min^{-1} of He for 30 min to flush out the excess NH_3. The reactor temperature then was raised to 800 °C at a rate of 10 °C min^{-1} in a flowing He of 30 mL min^{-1}.

A quartz vessel sealed with a rubber septum served as the photocatalytic reactor to examine the production of H_2 gas. Catalyst (40 mg) and ethanol (4.0 mL) are placed in the reactor and the suspension is purged with argon gas in an ice bath to prevent the evaporization of ethanol. The reactor was irradiated with two 15 W low-pressure mercury lamps (UVP, 365 nm) at room temperature and under argon atmosphere with magnetic stirring. After UV irradiation, 50 μL of gaseous products was collected and analyzed using a GC equipped with a TCD for gas analysis. The liquid phase suspension was centrifuged and a portion of the liquid was sampled and analyzed with another GC equipped with a FID for liquid product distribution.

3. Results and discussion

Figure 1 is the SEM image of the anatase TiO_2 powder starting material, which is composed of small particles with quite uniform diameter around 250 nm and a BET surface area around 10 m^2/g. Figure 2 shows the SEM image of TiO_2 nanotubes prepared after treating the anatase powder for 7 days in 10 M NaOH at 383 K. The long and tubular shape morphology of the nanotube is clearly visible in the figure, and more important, there is no TiO_2 particles (starting material) can be found. From our experience, as long as the reaction time in NaOH solution is sufficient all the TiO_2

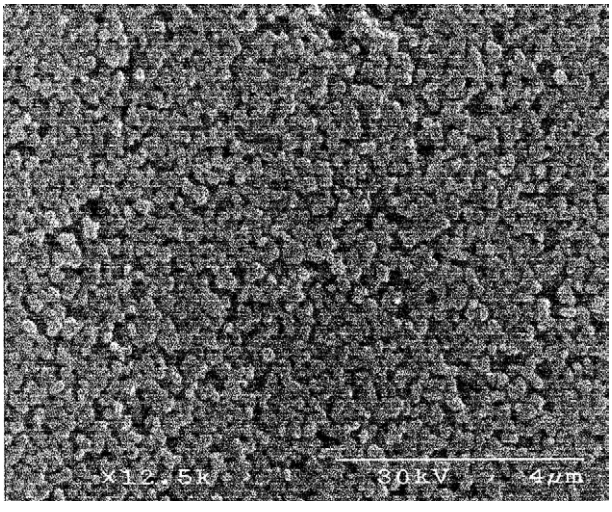

Figure 1. SEM image of anatase TiO_2 powder.

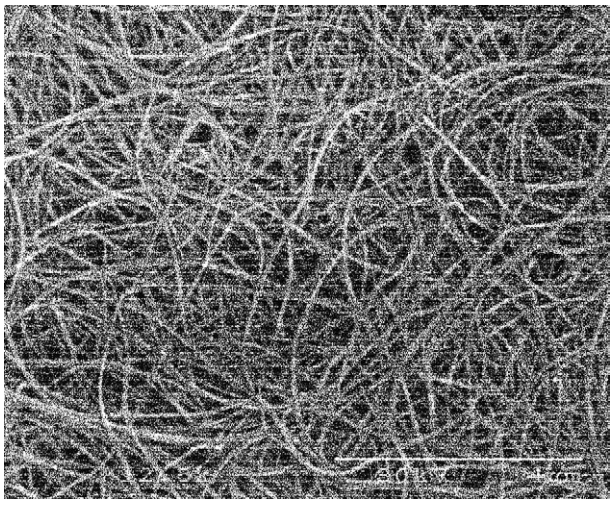

Figure 2. SEM image of TiO_2 nanotubes.

particles will ultimately be transformed into nanotubes, and the reaction product mixture will contain only pure TiO_2 nanotubes without visible particular starting material under SEM. Furthermore, it seems that if enough NaOH solution is made available to treat TiO_2 powder, there will be no limit on the amount of TiO2 nanotubes we can be prepared per synthesis run. Considering the high purity and easy availability as well as the superior structural properties mentioned above, this newly synthesized TiO_2 nanomaterial seems to be an excellent candidate to be utilized as a heterogeneous catalyst or as a catalyst support.

We had tested this TiO_2 nanotube as a heterogeneous photocatalyst for the dehydrogenation of ethanol to generate H_2 gas. The preliminary results indicated that this material was indeed able to produce H_2 gas from neat ethanol when irradiating with 365 nm UV light at ambient temperature under argon atmosphere. However, like other TiO_2 material it also needs to be promoted with Pt metal to enhance its photocatalytic activity for producing H_2 gas. As shown in figure 3, bare TiO_2 nanotubes, both washed with deionized H_2O or H_2SO_4 solution during preparation, produced almost no H_2. On the other hand, they started to produce a fair amount of H_2 gas (85 μmol at the 5th hour of reaction) once photodeposited with 1 wt% of Pt. Furthermore, higher Pt loading resulted in a more stable catalyst and produced more H_2 over tIlis Pt/TiO_2 nanotube catalyst. The data in figure 4 indicated that only catalyst with 1 wt % Pt loading was able to maintain the same H_2 production rate at the 5th hour of the reaction and produced more H_2 than the low Pt loading catalysts. The data implied that higher Pt loading is beneficial for both the catalyst activity and catalyst life, The UV-visible absorption spectra of Pt-promoted TiO_2 nanotube catalysts prepared by different methods (catalyst A–C; see below for the difference in these catalysts) were depicted in figure 5, which clearly indicated that these nanotube catalysts did absorb light in the UV region.

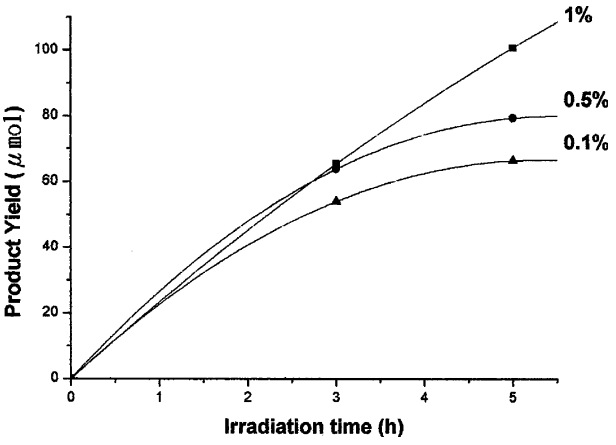

Figure 4. Hydrogen yields for TiO_2 nanotubes (H_2SO_4 washed and 573 K calcined) with different Pt loadings.

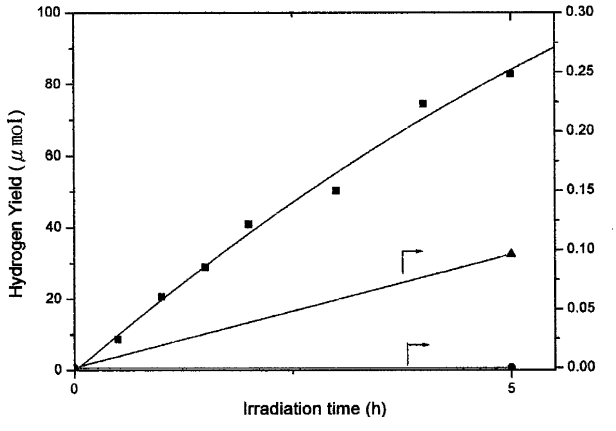

Figure 3. The hydrogen yields of different TiO_2 nanotubes dried at 383 K (■–H_2SO_4 washed and 1% Pt loading; ●–H_2O washed; ▲– – *H_{2}SO_{4}washed*).

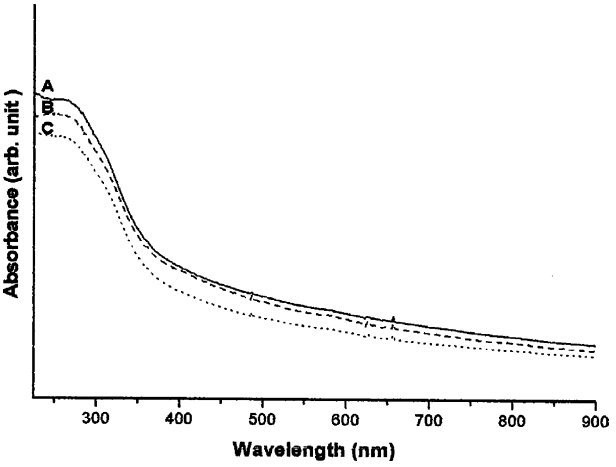

Figure 5. UV-visible spectra of 1% Pt/TiO_2 nanotube for catalyst A–C.

Many researchers had reported the beneficial effect of low-level Pt loading on H_2 production from alcohol. Pichat reported that higher initial H_2 production rates from primary alcohols over Pt/P-25 were for Pt content of 0.1–1 wt%, while catalysts with higher Pt contents (1–10 wt%) decreased the activity [19]. Teratani studied the photocatalytic dehydrogenation of aqueous 2-propanol over TiO_2 and a series of metal/TiO_2 powder [14]. He found that the order of the activity was the following: $Pt/TiO_2 > Rh/TiO_2 > Pd/TiO_2 > Ru/TiO_2 > Ir/TiO_2 > TiO_2$. For Pt/TiO_2, the initial reaction rate was proportional to Pt loading up to 0.5% and leveled off at higher loadings. Interestingly, the activities of all meta1/TiO_2 catalysts were enhanced upon heat treatment in air but the activity sequence was not altered.

Similarly, Ohtani observed that the H_2 production rate of photocatalytic dehydrogenation of 2-propanol in deaerated aqueous suspension of Degussa P-25 TiO_2, which is negligibly slow without Pt loading, increased drastically with the loading up to 0.3 wt% and slightly reduced with a further increase in Pt loading [20]. These researchers all agreed that the function of Pt was to attract the electrons generated by UV irradiation and prevented the recombination of the hole-electron pair in order to enhance the photocatalytic production of H_2.

In addition to Pt loading, we found that catalyst preparation procedure would influence significantly the H_2 production rate and the liquid phase product distribution. Figure 6 depicted the distribution of major reaction products over 1% Pt/TiO_2 nanotube (catalyst A). The order of preparation steps used to prepare this catalyst was washing nanotubes with 0.05 M H_2SO_4 (and dried at 383 K), calcination at 573 K and photodepostion of 1% Pt. In addition to H_2, acetaldehyde and 1, l-diethoxyethane (acetal) were found in the liquid phase. Other minor products observed were CO_2 (<0.1 μmol), methane (<0.2 μmol) and acetic acid (trace), which were not depicted in Figure 5. We rationalized such product distribution by equations (1–3).

$$CH_3CHO + 2C_2H_5OH \rightarrow CH_3CH(OC_2H_5)_2 + H_2O \quad (2)$$

$$CH_3CHO \rightarrow CH_3OOH \rightarrow CH_4 + CO_2 \quad (3)$$

Acetal was derived from the primary reaction product, acetaldehyde, by acid-catalyzed reaction (equation (2)) and acetic acid by further oxidation (equation (3)). We had shown that by impregnating TiO_2 nanotubes with H_2SO_4 solution followed by calcining at 573 K, these nanotubes would acquire some acidity and catalyzed the formation of acetal [6,21,22]. The decomposition of acetic acid into methane and CO_2 as reported by Bard *et al.* were thermodynamically favorable ($\Delta G^0 = -55.8$ kJ/mol) [23]. It should be noted that although acetal was formed over catalyst A, acetaldehyde was still the major liquid phase product during this reaction period.

It was surprising to discover that another 1% Pt/TiO_2 nanotube catalyst prepared by a different order (labeled as catalyst B) displayed an unexpected catalytic behavior. This catalyst was prepared by H_2SO_4 wash (and dried at 383 K), photodeposition of Pt, and calcination at 573 K. The product distribution of catalyst B was depicted in figure 7, in which significantly more H_2 gas was produced at the 5th hour of reaction than catalyst A (170 versus 107 μmol with catalyst A) and acetal became the dominant product in liquid phase (120 versus 50 μmol with catalyst A) over this catalyst. The effect of reversing the order of photodeposition of Pt and calcination steps was dramatic. Moreover, another catalyst labeled as catalyst C, prepared by washing the nanotubes with 0.10 M HCl, calcination at 573 K and photodeposition of Pt, produced 150 μmol of H_2 at the 5th hour of reaction. The ability of catalyst C to produce H_2 is significantly higher than catalyst A but lower than

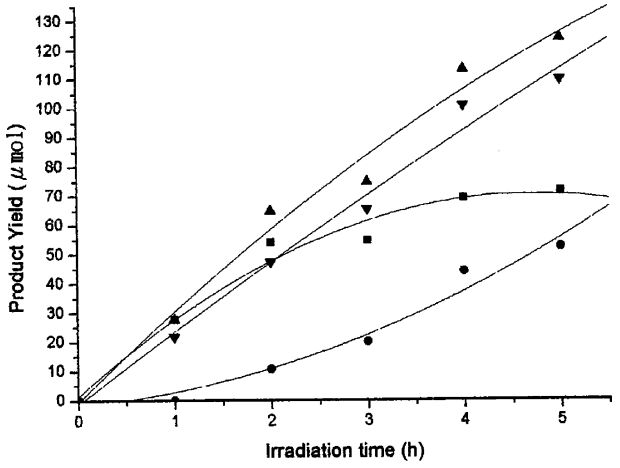

Figure 6. The product distribution over 1% Pt/TiO_2 nanotube (catalyst A) (■ – aldehyde; ● – acetal; – aldehyde + acetal; ▼ – H_2).

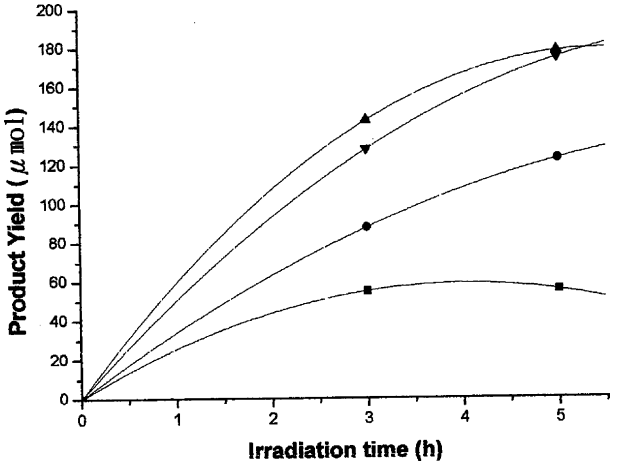

Figure 7. The product distribution over 1% Pt/TiO_2 nanotube (catalyst B) (■ – aldehyde; ● – acetal; ▲ – aldehyde + acetal; ▼ – H_2).

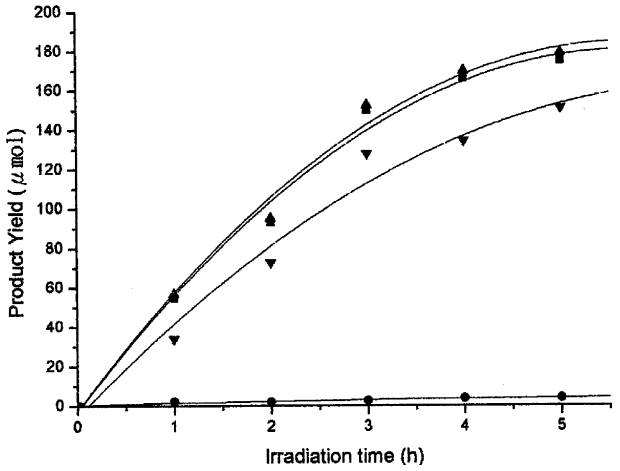

Figure 8. The product distribution over 1% Pt/TiO_2 nanotube (catalyst C) (■ – aldehyde; • – acetal; ▲ – aldehyde + acetal; ▼–H_2).

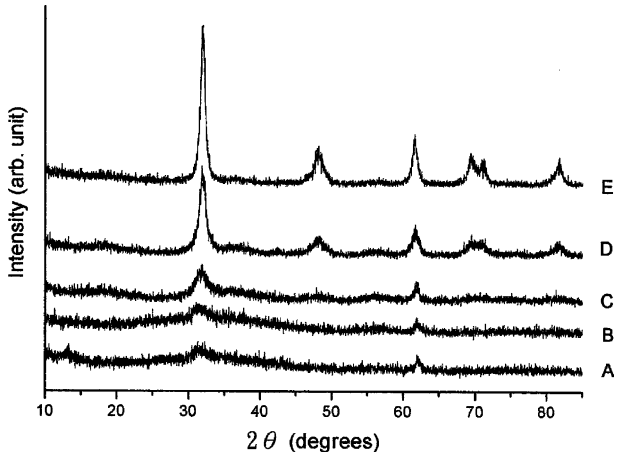

Figure 10. XRD spectra of TiO_2 nanotubes calcined at different temperatures (A) 383 K, (B) 473 K, (C) 573 K, (D) 673 K, (E) 773 K.

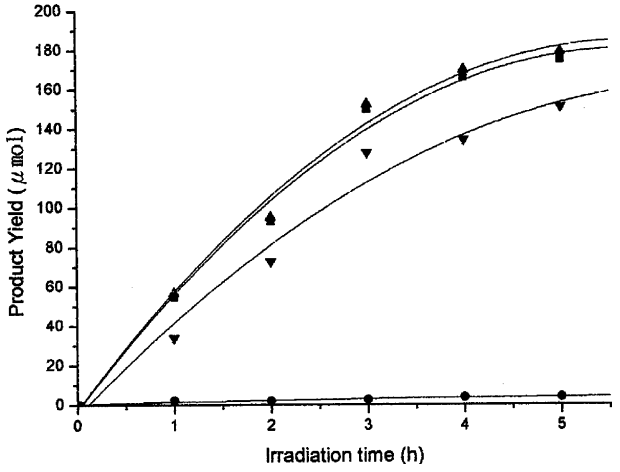

Figure 9. TPD/Mass spectra of catalyst A–C monitoring m/e = 16 of NH_3.

catalyst B. Interestingly, this catalyst C produced very small amount of acetal (see figure 8). It is obvious that washing TiO_2 nanotubes with different type of acidic solutions would affect the H_2 gas production rate and the production distribution of these Pt/TiO_2 nanotube catalysts.

We had measured the acid strength of these catalysts with TPD/MASS by monitoring the m/e = 16 of the NH_3 molecules as depicted in figure 9. The peak at m/e = 17 was not used because there was additional peak intensity contribution from the water molecules. As can be seen from figure 9, there is no significant difference in the strength of the acid sites among catalyst A–C but the order of the total number of the acid sites per unit catalyst weight measured by TPD/NH_3 was B>A >C. The total number of the acid sites in catalyst A–C were 112, 123 and 88 μmol g^{-1}, respectively. The higher concentration of the acid sites might assist in the formation of more acetal and in generating more H_2 gas by adapting a less energy-demanding reaction path (equation (4)). As water was produced in equation (4), this reaction path should be thermodynamically more favorabe.

$$3C_2H_5OH \rightarrow CH_3CH(OC_2H_5)_2 + H_2 + H_2O \qquad (4)$$

The effect of the calcination on the Pt metal dispersion and the crystallinity of TiO_2 should always not be neglected. Both effects resulted in better H_2 production activity. Calcination prior to reducing Pt ions to enhance H_2 production rate had been observed by Teratani and Bamwenda for Pt/TiO_2 catalysts prepared by photodeposition method [12,14] and in these cases, improving the metal dispersion should be the reason for the better activities. Calcination at 573 K also could improve the crystallinity of TiO_2 nanotubes. Figure 10 displayed the XRD spectra of the TiO_2 nanotubes (H_2SO_4 rinse) at different calcination temperatures. It clearly showed that at the low calcination temperatures of 383–473 K the crystallinity of the nanotubes was low as indicated by the appearance of the broad XRD diffraction peaks and only the (101) and (200) crystal planes of the anatase phase were present. The crystallinity of the catalyst continued to improve as the calcination temperature was increased to 573 K as (004) crystal plane started to develop. This was consistent with the data in Figures 3 and 4. In the fonner, 1% Pt/TiO_2 nanotubes were dried at 383 K produced 85 μmol of H_2 at the 5th hour and in the latter, the same catalyst calcined at 573 K produced 107 μmol of H_2 gas.

In summary, these activity and selectivity data strongly suggested that the photocatalytic behavior of these TiO_2 nanotube catalysts was greatly influenced by the preparation procedure and special cautions needed to be taken during the preparation of these nanotubular shape catalyst. We will continue to examine this Pt/TiO_2 photocatalyst in order to improve its performance and learn more about the structure-activity relationship from this new material.

Acknowledgments

The authors are grateful to Mr. J.-M. Ke, Misses M.-L. Zheng and X.-P. Wen for their assistances in spectroscopic measurements and the National Science Council of Taiwan, R.O.C. for a research grant (NSC 91-2113-M018-004) to support this research.

References

[1] G.A. Somorjai and Y.G. Borodko, Catal. Lett. 70 (2001) 1.
[2] H.H. Kung and M.C. Kung, Appl. Catal. A: Gen. 246 (2003) 193.
[3] D.A.H. Cunningham, W. Vogel, R.M.T. Sanchez, K. Tanaka and M. Haruta, J. Catal. 183 (1999) 24.
[4] G.H. Takaoka, T. Hamano, K. Fukushima, J. Matsuo and I. Yamada, Nucl. Instru. Meth. Phys. Res. B 121 (1997) 503.
[5] A. Fukuoka, N. Higashimoto, Y. Sakamoto, M. Sasaki, N. Sugimoto, S. Inagaki, Y. Fukushima and M. Ichikawa, Catal. Today 66 (2001) 21.
[6] C.-H. Lin, S.-H. Chien, J.-H. Chao, C.-Y. Sheu, Y.-C. Cheng, Y.-J. Huang and C.-H Tsai, Catal. Lett. 80 (2002) 153.
[7] C.-Y. Wang, J. Rabani, D.W. Bahnemann and J.K. Dohrmann, J. Photochem. Photobio. A: Chem. 148 (2002) 169.
[8] T. Kawahara, Y. Konishi, H. Tada, N. Tohge and S. Ito, Langmuir 17 (2001) 7442.
[9] K. Iseda, A. Towata, E. Watanabe, M. Fukaya and H. Taoda, Bull. Chem. Soc. Jpn. 71 (1998) 1249.
[10] K. Iseda, Bull. Chern. Soc. Jpn. 64 (1991) 1160.
[11] B. Ohtani, M. Kakimoto, S. Nishimoto and T. kagiya, J. Photochem. Photobio. A: Chem. 70 (1993) 265.
[12] G.R. Bamwanda, S. Tsubota, T. Nakamaru and M. Haruta, J. Photochem. Photobio. A: Chem. 89 (1995) 177.
[13] T. Sakata and T. Kawai, Chem. Phys. Lett. 80 (1981) 341.
[14] S. Teratani, J. Nakamichi, K. Taya and K. Tanaka, Bull. Chem. Soc. Jpn. 55 (1982) 1688.
[15] K. Domen, S. Naito, T. Takaharu Onishi and K. Tamaru, Chem. Lett. (1982) 555.
[16] S.I. Nishimoto, B. Ohtani, H. Shirai and T. Kagiya, J. Polym. Sci: Polym. Lett. Ed. 23 (1985) 141.
[17] S.I. Nishimoto, B. Ohtani, H. Shirai and T. Kagiya, J. Chem. Soc. Perkin Trans. II (1986) 661.
[18] S.I. Nishimoto, B. Ohtani and T. Kagiya, J. Chem. Soc. Faraday Trans. I 81 (1985) 2467.
[19] P. Pichat, M.N. Mozzanega, J. Disdier and J.M. Herrmamm, Nouv. J. Chim. 6 (1982) 559.
[20] B. Ohtani, K. Iwai, S.I. Nishimoto and S. Sato, J. Phys. Chem. B 31 (1997) 429.
[21] C.-H. Lin, S.-D. Lin, Y.-H. Yang and T.-P. Lin, Catal. Lett. 73 (2001) 121.
[22] C.-H. Lin, T.-P. Lin and Y.-J. Huang, Appl. Catal. A: Gen. 240 (2003) 253.
[23] B. Kraeutler and A.J. Bard, J. Phys. Chem. 83 (1979) 3146.